

## ORIGINAL ARTICLE

# An integrin antagonist (MK-0429) decreases proteinuria and renal fibrosis in the ZSF1 rat diabetic nephropathy model

Xiaoyan Zhou<sup>1</sup> , Ji Zhang<sup>2</sup>, Robin Haimbach<sup>2</sup>, Wei Zhu<sup>2</sup>, Rosemary Mayer-Ezell<sup>1</sup>, Margarita Garcia-Calvo<sup>1</sup>, Elizabeth Smith<sup>1</sup>, Olga Price<sup>1</sup>, Yanqing Kan<sup>2</sup>, Emanuel Zycband<sup>2</sup>, Yonghua Zhu<sup>2</sup>, Maarten Hoek<sup>2</sup>, Jason M. Cox<sup>3</sup>, Lijun Ma<sup>2</sup>, David E. Kelley<sup>2</sup> & Shirly Pinto<sup>2</sup>

<sup>1</sup>Department of Pharmacology, Merck & Co., Inc., 2000 Galloping Hill Road, Kenilworth, New Jersey 07033

<sup>2</sup>Department of Cardiometabolic Diseases, Merck & Co., Inc., 2000 Galloping Hill Road, Kenilworth, New Jersey 07033

<sup>3</sup>Department of Medicinal Chemistry, Merck & Co., Inc., 2000 Galloping Hill Road, Kenilworth, New Jersey 07033

## Keywords

Proteinuria, rat diabetic nephropathy model, renal fibrosis,  $\alpha v \beta 3$  integrin antagonist

## Correspondence

Xiaoyan Zhou, Department of Pharmacology, Merck Research Laboratories, 2000 Galloping Hill Road, Kenilworth, NJ 07033.

Tel: 908-740-4405; Fax: 908-740-4020;

E-mail: xiaoyan\_zhou@merck.com

and

Shirly Pinto, Kallyope, 430 East 29th St., New York, NY 10016. E-mail: pintoshirly@gmail.com

## Funding Information

Merck & Co., Inc.

Received: 13 June 2017; Revised: 13 July 2017; Accepted: 19 July 2017

*Pharma Res Per*, 5(5), 2017, e00354, <https://doi.org/10.1002/prp2.354>

doi: 10.1002/prp2.354

## Abstract

Multiple integrins have been implicated in modulating renal function. Modulation of integrin function can lead to pathophysiological processes associated with diabetic nephropathy such as alterations in the glomerular filtration barrier and kidney fibrosis. The complexity of these pathophysiological changes implies that multiple integrin subtypes might need to be targeted to ameliorate the progression of renal disease. To address this hypothesis, we investigated the effects of MK-0429, a compound that was originally developed as an  $\alpha v \beta 3$  inhibitor for the treatment of osteoporosis, on renal function and fibrosis. We demonstrated that MK-0429 is an equipotent pan-inhibitor of multiple  $\alpha v$  integrins. MK-0429 dose-dependently inhibited podocyte motility and also suppressed TGF- $\beta$ -induced fibrosis marker gene expression in kidney fibroblasts. Moreover, in the obese ZSF1 rat model of diabetic nephropathy, chronic treatment with MK-0429 resulted in significant reduction in proteinuria, kidney fibrosis, and collagen accumulation. In summary, our results suggest that inhibition of multiple integrin subtypes might lead to meaningful impact on proteinuria and renal fibrosis in diabetic nephropathy.

## Abbreviations

CKD, chronic kidney disease; Col IA1, collagen type I alpha-1 chain; CrCL, creatinine clearance; CTGF, connective tissue growth factor; DN, diabetic nephropathy; ECM, extracellular matrix; ESRD, end-stage renal disease; GFR, glomerular filtration rate; H&E, hematoxylin and eosin; HPKF, human primary kidney fibroblasts; LAP, latency-associated peptide; NHMC, normal human mesangial cells; PAI-1, plasminogen activator inhibitor-1; PAN, puromycin; PAS, periodic acid-Schiff; RGD, arginine-glycine-aspartic acid; RPTEC, human primary renal proximal tubule epithelial cells; TGF- $\beta$ , transforming growth factor beta; UPCr, urinary protein creatinine ratio; UUO, unilateral ureteral obstruction; VN, vitronectin;  $\alpha$ SMA,  $\alpha$ -smooth muscle actin.

## Introduction

Diabetic nephropathy (DN) is the leading cause of end-stage renal disease (ESRD) in the United States (Afkarian et al. 2013; USRDS ADR, 2014). However, a complete understanding of the pathogenesis of DN at the molecular level is still lacking, although numerous hypotheses,

including reactive oxygen species, nitric oxide, transforming growth factor beta (TGF- $\beta$ ), inflammatory cytokines, and endothelin, have been proposed and are being evaluated preclinically and clinically (Arora and Singh 2013; Gentile et al. 2014; Breyer and Susztak 2016).

Emerging evidence has demonstrated that integrins play a critical role in kidney diseases (Pozzi and Zent 2013).

Integrins are cell surface protein receptors composed of  $\alpha$  and  $\beta$  subunits, participating in multiple cellular functions such as adhesion and anchoring to extracellular matrix (ECM), and transducing growth factor signals (Pozzi and Zent 2013). There are 24 unique integrin heterodimers, many of which have been shown to be upregulated in diabetic kidneys (Jin et al. 1996). Although multiple integrins are associated with DN, we focused our attention on evaluating the role of the arginine-glycine-aspartic acid (RGD)-binding  $\alpha v$  heterodimers. The  $\alpha v$  integrins primarily interact with the RGD sequence present in fibronectin ( $\alpha v \beta 1$  and  $\alpha 5 \beta 1$ ) and vitronectin ( $\alpha v \beta 3$  and  $\alpha v \beta 5$ ) or TGF- $\beta$  latency-associated peptide (LAP) ( $\alpha v \beta 1$ ,  $\alpha v \beta 6$ , and  $\alpha v \beta 8$ ) (Munger et al. 1999; Hynes 2002; Kitamura et al. 2011; Reed et al. 2015).  $\alpha v$  integrins play a key role in the activation of latent TGF- $\beta$  (Henderson and Sheppard 2013). Dysregulated expression and response to TGF- $\beta$  has been implicated in a wide variety of disease processes including fibrotic disease and chronic inflammation (Akhurst and Hata 2012; Ding and Choi 2014). Although the role of RGD integrins in the kidney has not been tested in the clinic, preclinical evidence suggests that modulating  $\alpha v$  integrin activity could lead to protective effects in multiple tissues. It has been shown that Pdgfrb-Cre-mediated depletion of  $\alpha v$  integrin leads to protection against hepatic fibrosis induced by CCL4, renal fibrosis induced by unilateral ureteral obstruction (UUO), and lung fibrosis induced by bleomycin (Henderson et al. 2013). A small molecule RGD mimetic CWHM12 accordingly attenuated liver and lung fibrosis (Henderson et al. 2013). Deletion of  $\beta 6$  integrin in mice is protective against UUO-induced renal fibrosis (Ma et al. 2003) and bleomycin-induced lung fibrosis (Munger et al. 1999). An  $\alpha v \beta 6$  neutralizing antibody has shown similar effect in lung fibrosis (Horan et al. 2008) and is currently being tested in phase II trials for the treatment of idiopathic pulmonary fibrosis.  $\alpha v \beta 3$  has been proposed to play a role in regulating glomerular filtration barrier and podocyte injury response by a mechanism partially through the urokinase plasminogen receptor (Wei et al. 2008). Furthermore, an  $\alpha v \beta 3$  integrin antibody has been shown to prevent the development of DN in diabetic pigs (Maile et al. 2014a) and diabetic rats (Maile et al. 2014b).

The complexity of the integrins and their role in the progression of disease suggest that pharmacological inhibition of multiple integrin subtypes may be required to lead to meaningful effects on delaying the progression of DN. Hence, we characterized the selectivity, potency, and function of MK-0429 on multiple integrins; this compound was originally developed as an  $\alpha v \beta 3$  inhibitor for osteoporosis treatment and was well tolerated in Phase II trials (Hutchinson et al. 2003; Coleman et al. 2004;

Murphy et al. 2005; Rosenthal et al. 2010). We also assessed the effects of MK-0429 on renal function and fibrosis in the ZSF1 rat model of DN.

## Materials and Methods

### Cultured cells and reagents

Human primary kidney fibroblasts (HPKF, from CellBiologics), human primary renal proximal tubule epithelial cells (RPTEC, from Lonza), and normal human mesangial cells (NHMC, from Lonza) were cultured at 37°C in the presence of 5% CO<sub>2</sub>. Conditionally immortalized human podocyte cell line AB8/13 (provided by Professor Moin Saleem, University of Bristol, UK) was used to assess podocyte motility. To induce a fibrotic response in primary cells, a final concentration of 5 ng/mL of recombinant human TGF- $\beta 1$  (BioLegends) was added to the culture media and treated for 24 h. MK-0429 (L-000845704) was synthesized by Merck & Co., Inc., Kenilworth, NJ, USA, enalapril was purchased from Sigma-Aldrich (St. Louis, Missouri).

### Solid-phase receptor assay

The assay was performed according to the method previously described (Patent WO 2014/015054 A1 "Beta Amino Acid Derivatives As Integrin Antagonists"). The IC<sub>50</sub> value was obtained from two to three different experiments.

### Thermal shift assay

Differential scanning fluorimetry was performed on a LightCycler 480 II, real-time PCR instrument (Roche Diagnostics, Indianapolis, IN). Human recombinant  $\alpha 1 \beta 1$ ,  $\alpha 2 \beta 1$ ,  $\alpha 3 \beta 1$ ,  $\alpha 4 \beta 1$ ,  $\alpha 6 \beta 1$ ,  $\alpha 9 \beta 1$ ,  $\alpha 10 \beta 1$ ,  $\alpha 11 \beta 1$ , and  $\alpha I I b \beta 3$  integrins from R&D Systems were reconstituted in assay buffer and Sypro orange (Sigma-Aldrich, St. Louis, MO). Twenty  $\mu$ M of MK-0429 was added to the mixture of protein and dye by using a Labcyte Echo 555 instrument. Changes in protein thermal stability ( $\Delta T_m$ ) upon compound binding were analyzed by using LightCycler 480 software provided by the manufacturer. All assays were performed in triplicate and the results were obtained from three independent experiments.

### Integrin coimmunoprecipitation and western blot analyses

Cells or kidney tissue were lysed with lysis buffer. Cell lysates were incubated with anti- $\alpha v$  antibody (L230, Enzo) and Protein G magnetic beads (Pierce). The supernatant

was subsequently subjected for Sally Sue simple western analysis (ProteinSimple, San Jose, CA). The antibodies used for detecting  $\beta 1$ ,  $\beta 3$ , and  $\beta 5$  integrins were from Abcam, anti- $\beta 6$  integrin antibody was from R&D Systems, and anti-GAPDH antibody was from Cell Signaling Transduction.

### Kidney fibroblast fibrosis assay

Human primary kidney fibroblasts (HPKF) were plated in Collagen I-coated 96-well plate. After serum starvation overnight, the cells were treated with various concentrations of MK-0429 for 24 h. For those cells treated with TGF- $\beta$ , compound was added 1 h prior to TGF- $\beta$  treatment. RNA was subsequently extracted and followed by reverse transcription reaction and real-time PCR analysis (ABI 7900HT).

### Podocyte motility assay

Studies were performed when human podocytes were fully differentiated 10 days after thermoswitching. The effect of MK-0429 on human podocyte motility was examined using Oris cell migration assay in vitronectin-coated 96-well plate. Cells were exposed to Puromycin (15  $\mu\text{g}/\text{mL}$ ) for 48 h in the presence or absence of MK-0429 at different concentrations. Plates were scanned by the acumen Cellista (TTP Labtech, Melbourne UK) to capture whole well images.

### Animals

Male ZSF1 rats (a hybrid F1 of Zucker diabetic fatty rat and spontaneously hypertensive heart failure rat) (Charles River Laboratories, Wilmington, MA) were housed in a temperature- and humidity-controlled facility with a 12-h light: 12-h dark, light cycle. Animals had ad libitum access to food (Purina Rodent Chow 5053, LabDiet, St. Louis, MO) and water. The medicated diets (either MK-0429 or enalapril mixed in Purina Rodent Chow 5053) were prepared by Research Diets, Inc. (New Brunswick, New Jersey). All procedures utilizing experimental animals were conducted in accordance with the Guide for the Care and Use of Laboratory Animals as adopted and promulgated by the U.S. National Institutes of Health, and experimental procedures were reviewed and approved by the Institutional Animal Care and Use Committee at Merck & Co., Inc., Kenilworth, NJ.

### In vivo experimental protocol

Sixty obese male ZSF1 rats were randomized by 24-h protein/creatinine ratio at baseline to five groups: Obese

control ( $n = 12$ ), MK-0429 60 mg/kg/day ( $n = 12$ ), MK-0429 200 mg/kg/day ( $n = 12$ ), MK-0429 400 mg/kg/day ( $n = 12$ ), enalapril 10 mg/kg/day ( $n = 12$ ); Eight lean male ZSF1 rats were used for normal control. Baseline values were collected at 14 weeks of age. Treatment started at 16 weeks of age and continued for 28 weeks. Treatment groups received medicated diet; compound in feed concentration was determined by body weight and daily food intake. Lean and obese control groups received control diet. Blood and urine were collected at week  $-2$ , 1, 2, 4, 6, 8, 12, 16, 21, 24, and 28.

### Renal function and blood biochemistry monitoring

All rats were acclimated to single housing in metabolic cages with free access to food and water for at least 3 days prior to urine and blood collection. Blood samples and 24-h urine were collected at various time points. Urine and blood samples were then centrifuged, portioned in aliquots, and frozen at  $-80^{\circ}\text{C}$  until analyzed. Rats were weighed, food and water consumption were recorded at the same time on each occasion of urine and blood collection throughout the study. Plasma creatinine was measured by mass spectrometry (Sciex, Framingham, Massachusetts). Urinary protein and creatinine were measured by a Roche Modular Chemistry System (Roche Diagnostics, Indianapolis, IN). GFR was estimated by creatinine clearance (CrCL) and measured by FITC-sinistrin clearance. For FITC-sinistrin clearance, a miniaturized device (NIC-Kidney, Mannheim Pharma & Diagnostics, Mannheim, Germany) was used as previously described (Schock-Kusch et al. 2011; Cowley et al. 2013).

### Kidney histology

Upon completion of the study, animals were sacrificed and kidneys were collected for histology assessment. Kidney tissues were fixed in 10% formalin and then paraffin embedded. Tissue sections were stained with hematoxylin and eosin (H&E), periodic acid-Schiff (PAS), and Masson's trichrome and evaluated under light microscope. The severity of histopathological changes in renal tubules, interstitium, vasculature, and glomeruli were graded on a 0–5 scale corresponding to normal, minimal, mild, moderate, marked, and severe as described previously (Zhou et al. 2011, 2013). Sections from both kidneys were examined. Collagen deposition in the kidney was graded on a 0–5 scale corresponding to normal, minimal, mild, moderate, marked, and severe, based on the blue stained area size and intensity. Following deparaffinization and rehydration, each kidney tissue section was processed to identify collagen I and III deposition. The primary antibodies

used were rabbit anti-type I collagen polyclonal antibody (Abcam, Cambridge, MA) diluted at 2  $\mu\text{g}/\text{mL}$ , and rabbit anti-type III collagen polyclonal antibody (Lifespan, Seattle, WA) at 3  $\mu\text{g}/\text{mL}$ . The signal was developed using Super PicTure HRP Polymer Rabbit Primary kit (Invitrogen) and the slides were counterstained with hematoxylin. The Aperio ScanScope XT Slide Scanner (Aperio Technologies, Vista, CA) system was used to capture whole slide digital images with a 20 $\times$  objective. Digital images were managed using Aperio Spectrum. The positive stains were identified and quantified using a macro created from a color deconvolution algorithm (Aperio Technologies, Vista, CA).

### RT-PCR and gene expression analysis

Kidney cortexes were extracted from control and experimental animals and immediately snap-frozen in liquid nitrogen and stored at  $-80^{\circ}\text{C}$  until used. TRIzol (Life technologies, Carlsbad, CA) was used to homogenize the samples. Total RNA was extracted following the instruction of RNeasy Mini QIAcube Kit (Qiagen, Hilden, Germany). Two microgram RNA was then reverse-transcribed using SuperScript VILO cDNA Synthesis kit (Life technologies, Carlsbad, CA). Two microliter-diluted cDNA was added to quantitative real-time PCR mix with TaqMan Universal

PCR Master mix (Applied Biosystems, Foster City, CA) and rat Taqman probe (Life Technologies, Carlsbad, CA). PCR amplification was done in an Applied Biosystems 7900HT Fast Real-Time PCR System (Applied Biosystems, Foster City, CA) using rat POLR2A and B2M as an internal control. Ct of each sample was normalized to geomean of POLR2A and B2M levels and quantified based on 2 $e^{-\Delta\Delta\text{Ct}}$  method (comparing with obese vehicle group).

### Statistical analysis

All data are presented as mean  $\pm$  standard error of the mean (SE). Two-way or one-way ANOVA post hoc Tukey or *t*-test was used for longitudinal or one single time point data comparisons, respectively. All analyses were done using Prism 7 software. A *P* value of  $<0.05$  was considered to be statistically significant.

## Results

### MK-0429 is a potent pan- $\alpha v$ integrin antagonist

To determine selectivity of MK-0429 on integrins without being biased by the relative abundance of each integrin in the assay system, we performed solid-phase ELISA assays and compared the ability of MK-0429 to inhibit the binding of recombinant soluble integrin proteins to immobilized ligands. Different ligands and optimized assay conditions were used for each integrin to obtain curve-fitted  $\text{IC}_{50}$  value for MK-0429 (dose-titration plots were shown in Fig. S1A). As shown in Table 1, MK-0429 had potent activity against  $\alpha v\beta 1$  ( $\text{IC}_{50} = 1.6 \text{ nmol/L}$ ),  $\alpha v\beta 3$  ( $\text{IC}_{50} = 2.8 \text{ nmol/L}$ ),  $\alpha v\beta 5$  ( $\text{IC}_{50} = 0.1 \text{ nmol/L}$ ),  $\alpha v\beta 6$  ( $\text{IC}_{50} = 0.7 \text{ nmol/L}$ ),  $\alpha v\beta 8$  ( $\text{IC}_{50} = 0.5 \text{ nmol/L}$ ), and  $\alpha 5\beta 1$  ( $\text{IC}_{50} = 12.2 \text{ nmol/L}$ ), making it a rather nonselective inhibitor for all  $\alpha v$  integrins. Alpha5 and  $\alpha v$  integrins share considerable sequence similarity, especially around the RGD-binding pocket. Thus, it is not surprising that MK-0429 also strongly inhibited the binding of  $\alpha 5\beta 1$  to its ligand fibronectin. We next expanded our evaluation of

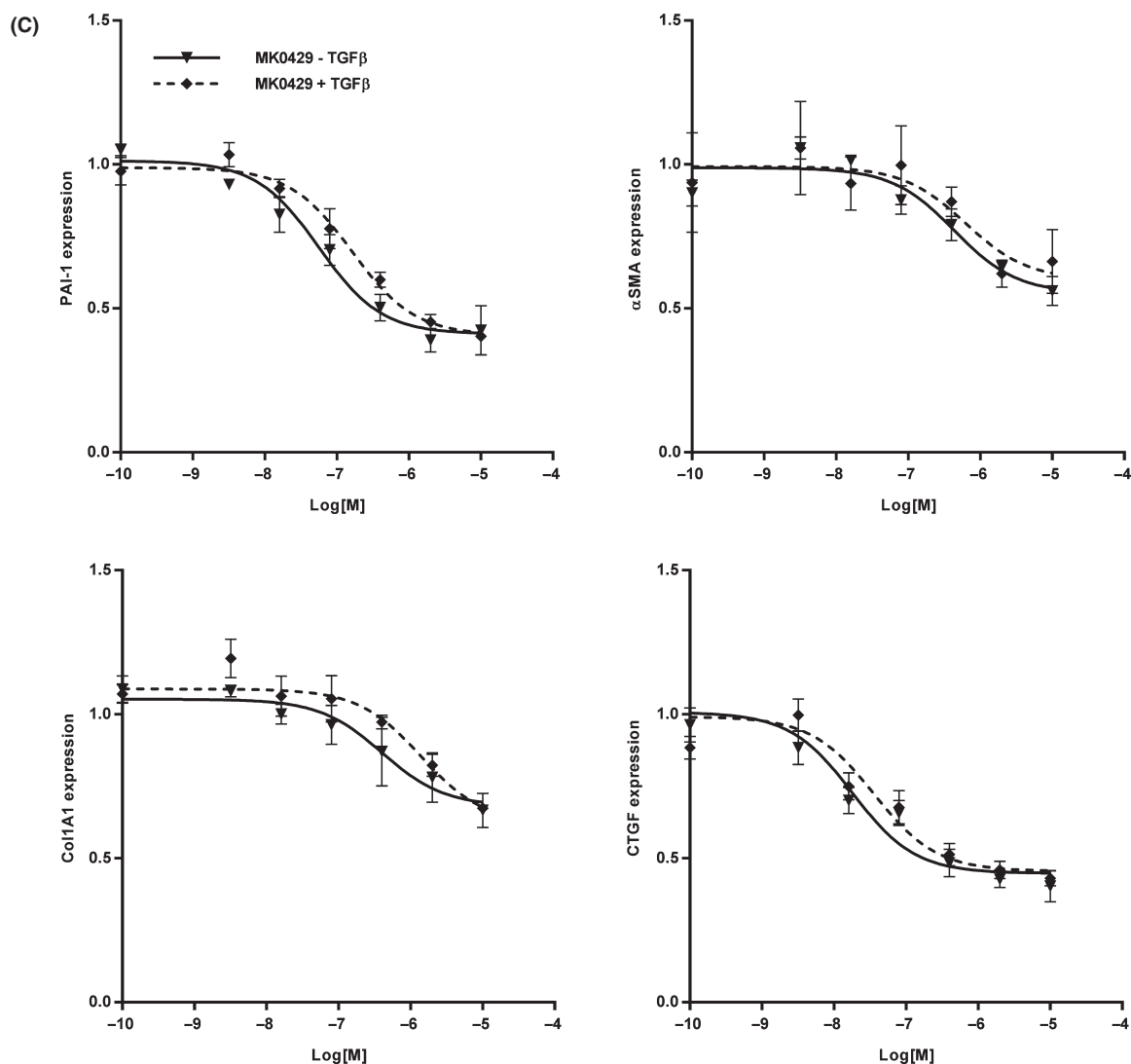
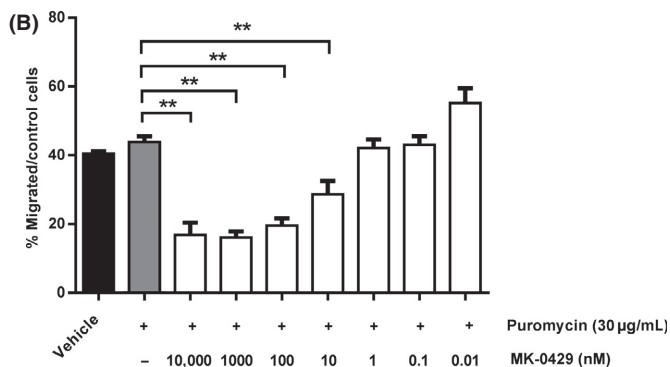
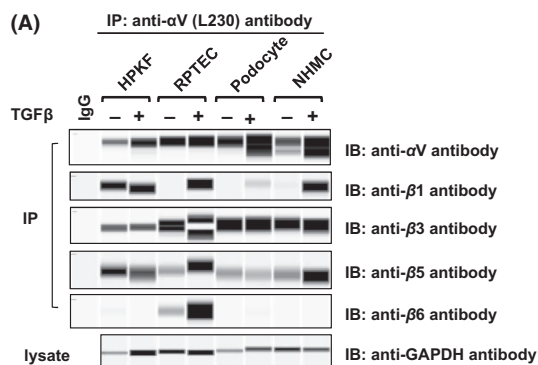
**Table 1.** In vitro selectivity of MK-0429 against various integrin subtypes.

$\text{IC}_{50}$ on various integrin	MK-0429
$\alpha v\beta 1$ – inhibition of fibronectin-binding $\text{IC}_{50}$ (nmol/L)	$1.6 \pm 0.7$
$\alpha v\beta 3$ – inhibition of vitronectin-binding $\text{IC}_{50}$ (nmol/L)	$2.8 \pm 3.4$
$\alpha v\beta 5$ – inhibition of vitronectin-binding $\text{IC}_{50}$ (nmol/L)	$0.1 \pm 0.1$
$\alpha v\beta 6$ – inhibition of LAP-binding $\text{IC}_{50}$ (nmol/L)	$0.7 \pm 0.5$
$\alpha v\beta 8$ – inhibition of LAP-binding $\text{IC}_{50}$ (nmol/L)	$0.5 \pm 0.2$
$\alpha 5\beta 1$ – inhibition of fibronectin-binding $\text{IC}_{50}$ (nmol/L)	$12.2 \pm 10.4$
Binding to other integrins – $\alpha 1\beta 1$ , $\alpha 2\beta 1$ , $\alpha 3\beta 1$ , $\alpha 4\beta 1$ , $\alpha 6\beta 1$ , $\alpha 9\beta 1$ , $\alpha 10\beta 1$ , $\alpha 11\beta 1$ , and $\alpha \text{II} \beta 3$ <sup>1</sup>	No

Mean  $\pm$  SD from three independent experiments is shown.

<sup>1</sup>Binding of MK-0429 to each integrin was determined by thermal shift assay.

**Figure 1.** (A) The expression of various integrins in primary human kidney cells. Following immunoprecipitation with an anti- $\alpha v$  antibody, the  $\alpha v\beta 1$ ,  $\alpha v\beta 3$ ,  $\alpha v\beta 5$ , and  $\alpha v\beta 6$  heterodimers were detected by automated western analysis using antibodies that recognize the individual  $\beta$ -subunit. GAPDH level in total cell lysate was used as loading control. Human primary kidney fibroblasts (HPKF), human primary renal proximal tubule epithelial cells (RPTEC), and normal human mesangial cells (NHMC). IP, immunoprecipitation; IB, immunoblotting. (B) MK-0429 inhibits podocyte motility in Oris cell migration assay. Cells were exposed to puromycin (PAN, 15  $\mu\text{g}/\text{mL}$ ) for 24 h in the presence or absence of MK-0429 at different concentrations (ranging from 0.01 nmol/L to 10  $\mu\text{mol/L}$ ,  $n = 8$  for each concentration).  $***P < 0.01$ , one-way ANOVA. (C) MK-0429 suppresses the expression of fibrosis marker genes in HPKFs under basal condition or upon TGF- $\beta$  stimulation ( $n = 8$  for each group). PAI-1, plasminogen activator inhibitor-1;  $\alpha\text{SMA}$ ,  $\alpha$ -smooth muscle actin; Col IA1, Collagen type I alpha-1 chain; CTGF, connective tissue growth factor.



MK-0429 selectivity profile to other  $\beta 1$ -containing integrins by thermal shift assay. Compared to solid-phase ELISA which measures integrin-ligand interaction, the thermal shift assay directly assesses the binding of compound (MK-0429) to each integrin. The addition of

MK-0429 to  $\alpha v\beta x$  integrins caused dramatic shift of melting temperatures (Fig. S1B), suggesting strong compound-protein interaction. This is consistent with the nmol/L potency of MK-0429 observed in inhibition  $\alpha v\beta x$  integrin-ligand binding in solid-phase ELISA.

Furthermore, we examined the binding of MK-0429 to recombinant human  $\alpha 1\beta 1$ ,  $\alpha 2\beta 1$ ,  $\alpha 3\beta 1$ ,  $\alpha 4\beta 1$ ,  $\alpha 6\beta 1$ ,  $\alpha 9\beta 1$ ,  $\alpha 10\beta 1$ ,  $\alpha 11\beta 1$ , or  $\alpha IIb\beta 3$  integrin. MK-0429 caused minimal change in their melting temperatures, suggesting that MK-0429 does not bind to any of these integrins and is unlikely to affect their functions. Taken together, these results demonstrate that MK-0429 is a potent pan- $\alpha v$  integrin antagonist.

### Expression of $\alpha v$ integrin subtypes in various renal cell types

To better understand the function of  $\alpha v$  integrins in the kidney, we examined the expression of all  $\alpha v$  integrins in human primary kidney fibroblasts (HPKF), human primary renal proximal tubule epithelial cells (RPTEC), podocytes, and normal human mesangial cells (NHMC). The total pool of  $\alpha v$  integrins was first immunoprecipitated from the cell lysates and subsequently blotted for the abundance of each  $\beta$  subunit. As shown in Figure 1A and densitometry graph (Fig. S1C), the expression of  $\alpha v\beta 6$  integrin was restricted to RPTEC and was further induced by TGF- $\beta$  stimulation. Meanwhile,  $\alpha v\beta 3$  and  $\alpha v\beta 5$  were more broadly expressed in various kidney cell types (Fig. 1A).  $\alpha v\beta 1$  was readily detected in HPKF, while it was only found after TGF- $\beta$  treatment in RPTEC, podocytes, and NHMC (Fig. 1A). In podocytes, the  $\alpha v$  integrin was upregulated upon TGF- $\beta$  treatment, densitometry analysis further revealed increased  $\alpha v\beta 1$ ,  $\alpha v\beta 3$ , and  $\alpha v\beta 5$  expression, suggesting important roles for those integrin in podocyte biology.

### MK-0429 affects podocyte motility and fibrosis response in kidney fibroblasts

To evaluate the cellular effect of MK-0429 on podocyte plasticity, we examined the migration of podocytes on vitronectin-coated surface. Puromycin has been commonly used to induce podocyte injury and cause proteinuria in vivo (Kindt *et al.* 2017). Puromycin-treated human podocytes displayed a slight increase in cell motility, compared to untreated vehicle groups. MK-0429 treatment for 48 h inhibited the puromycin-induced podocyte motility in a dose-dependent manner, with an  $IC_{50}$  of 9.9 nmol/L (Fig. 1B), without affecting cell viability (unpublished data, X.Z., J.Z., R.H., W.Z., R.M.E., M. G.C., E.S., O.P., Y.K., E.Z., Y.Z., M.H., J.M.C., L.M., D.E.K., S.P.).  $\alpha v\beta 3$  and  $\alpha v\beta 5$  integrins are abundant in podocytes (Fig. 1A and Fig. S1C). As a pan- $\alpha v$  antagonist, MK-0429 likely functions through these integrins to modulate cell motility on vitronectin. To probe the potential role of MK-0429 in kidney fibroblasts, cells were treated with MK-0429 at various concentrations and the

expression of fibrosis marker genes  $\pm$  TGF- $\beta$  was subsequently examined.

In HPKF, plasminogen activator inhibitor-1 (PAI-1) mRNA expression was not further induced by TGF- $\beta$  (Fig. 1C), indicating that these kidney fibroblasts were already activated. In the absence or presence of TGF- $\beta$ , MK-0429 inhibited PAI-1 gene expression with  $IC_{50}$  at 56.5 nmol/L and 163 nmol/L, respectively. In addition to PAI-1, MK-0429 also strongly suppressed the expression of connective tissue growth factor (CTGF), and partially inhibited  $\alpha$ -smooth muscle actin ( $\alpha$ SMA) and Collagen type I alpha-1 chain (Col IA1) (Fig. 1C).

### Upregulation of $\alpha v$ integrins in ZSF1 rat

The obese ZSF1 rat exhibits hyperglycemia, hypertension, and hyperlipidemia, and features of DN in humans (Tofovic *et al.* 2000; Zhang *et al.* 2007). It has been widely accepted as an experimental model of DN. To determine the expression of  $\alpha v$  integrins in the ZSF1 rat, we carried out automated western analysis of total kidney extracts ( $n = 5$  in lean and obese group). As shown in Figure 2A and B, the relative abundance of  $\alpha v$ ,  $\beta 1$ ,  $\beta 3$ ,  $\beta 5$ , and  $\beta 6$  integrins was significantly upregulated when DN was evident. In particular, the upregulation of  $\beta 3$  and  $\beta 5$  integrin was more pronounced ( $P < 0.01$ ), compared to age-matched lean animals.

### Effects of MK-0429 on renal function and fibrosis in ZSF1 rat

In this study, obese ZSF1 rats showed significant proteinuria at 16 weeks of age and the proteinuria progressively increased over time (Fig. 3). Glomerular filtration rate (GFR), either estimated by creatinine clearance (CrCL) or measured by FITC-sinistrin clearance, was reduced by >50% at the completion of the study at 44 weeks of age (Fig. 4A and B). Enalapril (10 mg/kg/day) treatment significantly decreased urinary protein/creatinine ratio (UPCR) throughout the course of the study. MK-0429 (400 mg/kg/day) treatment induced a significantly later onset in its effects to reduce in UPCR (Fig. 3), suggesting its mechanism is distinct from enalapril. MK-0429 had no significant effect on GFR (Fig. 4). MK-0429 had no significant effects on body weight, food intake, and water intake in ZSF1 rats (Data not shown). Although MK-0429 had no significant effect on glomerular and tubular injury scores (data not shown), 400 mg/kg/day of MK-0429 did significantly decrease tubulointerstitial fibrosis as assessed by collagen deposition based on Masson's trichrome staining (Fig. 5A and B). Expression of collagen I and III protein in the kidney was also significantly decreased by MK-0429 (400 mg/kg/day) (Fig. 6A and B). It is worthwhile to

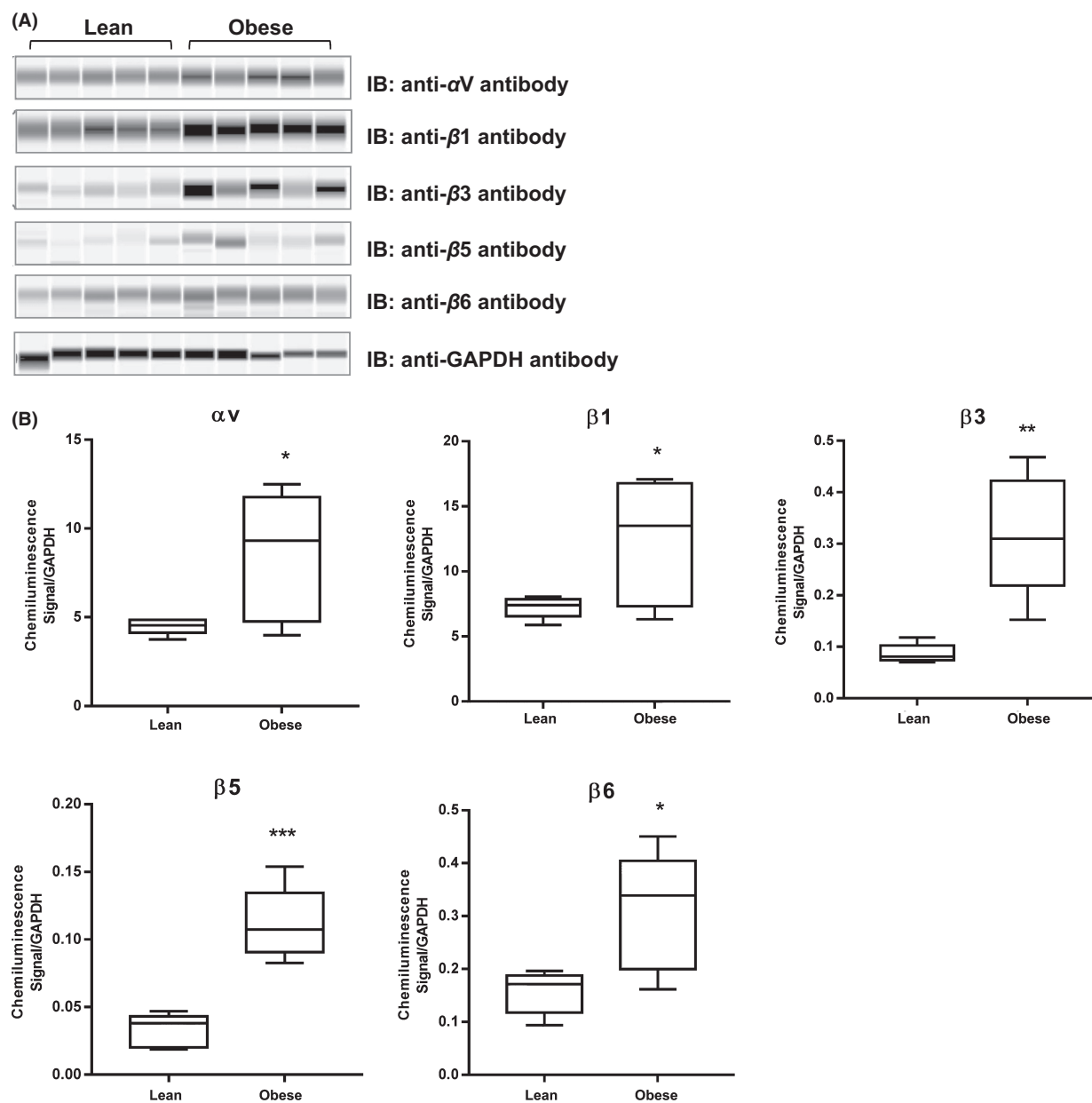


**Figure 2.** (A) The expression of each integrin in lean or obese ZSF1 rats at 30 weeks of age was determined by automated western analysis using antibodies that recognize the individual  $\alpha$  or  $\beta$ -subunit. GAPDH level in total kidney lysate was used as loading control. (B) Relative chemiluminescent intensity of each integrin was normalized to that of GAPDH in each animal.  $n = 5$ , \* $P < 0.05$ , \*\* $P < 0.01$ , \*\*\* $P < 0.005$ ,  $t$ -test.

mention that the renal histological change (including fibrosis) was normal in the lean ZSF1 rats; therefore, the treatment groups were compared to the obese ZSF1 rats.

### Effects of MK-0429 on expression of profibrotic genes

mRNA expression of Col I A1, Col III A1, PAI-1, and  $\alpha$ SMA was significantly increased in the kidneys of obese ZSF1 rats, and significantly decreased by MK-0429 treatment (Fig. 7).

The effect of MK-0429 on the mRNA expression of the above-mentioned fibrotic markers from our in vivo study is consistent with the findings from the in vitro kidney fibroblast assay, which likely defines the mechanism of MK-0429-decreased kidney tubulointerstitial fibrosis.

### Discussion

In this study, we examined the effects of chronic treatment of MK-0429, a potent small molecule pan- $\alpha$ v

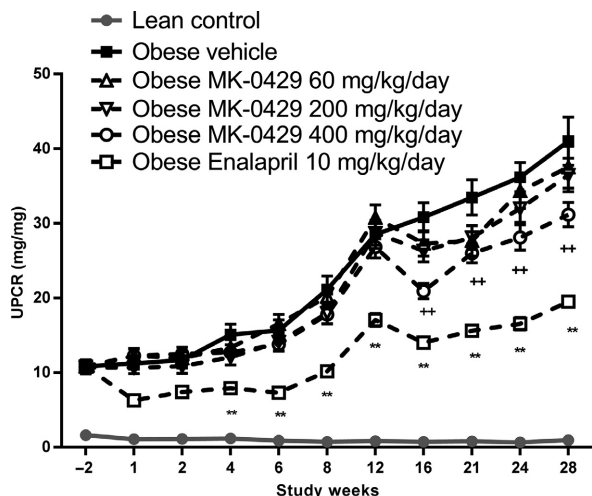


**Figure 3.** Time course of urinary protein to creatinine ratio (UPCR) in all groups. Data are mean  $\pm$  SEM ( $n = 8$  for the lean control group,  $n = 12$  for all the obese groups with or without treatment).  $**P < 0.01$ , enalapril 10 mg/kg/day versus obese vehicle.  $**P < 0.01$ , MK-0429 400 mg/kg/day versus obese vehicle (two-way ANOVA followed by Tukey).

integrin inhibitor, on renal function and fibrosis in the ZSF1 rat, an established model of DN. Our data demonstrate that 400 mg/kg/day of MK-0429 treatment led to late onset of anti-proteinuric and anti-fibrotic effects.

MK-0429 is an orally active, potent molecule, originally developed as an inhibitor of  $\alpha v\beta 3$  integrin to treat

osteoporosis (Hutchinson et al. 2003; Coleman et al. 2004; Murphy et al. 2005; Rosenthal et al. 2010). MK-0429 was tested in a randomized phase II trial in postmenopausal women with osteoporosis; it led to improvement of multiple endpoints including bone mineral density at spine and hip (Murphy et al. 2005). MK-0429 was also tested in a small clinical study in men with hormone-refractory prostate cancer and bone metastases where it significantly reduced bone turnover (Rosenthal et al. 2010). MK-0429 was initially designed as an RGD mimetic that incorporates key pharmacophores of guanidine and carboxylic acid of the RGD tripeptide sequence, followed by extensive molecule optimization efforts. In addition to  $\alpha v\beta 3$ , several other integrins are also known binders to the RGD sequence, including  $\alpha IIb\beta 3$ ,  $\alpha v\beta 1$ ,  $\alpha v\beta 5$ ,  $\alpha v\beta 6$ ,  $\alpha v\beta 8$ ,  $\alpha 5\beta 1$ , and  $\alpha 8\beta 1$  (Hynes 2002). As such, it is of importance to determine the selectivity of MK-0429 against other RGD-binding integrins. Our previous studies have found that MK-0429 inhibits  $\alpha v\beta 3$  ligand binding and osteoplastic bone resorption while remaining inactive in a platelet aggregation assay (Hutchinson et al. 2003). In the present work, we sought to assess the selectivity profile of MK-0429 against a broader collection of integrin proteins and found that MK-0429 is a pan RGD inhibitor.

There are extensive data implicating various integrins in the progression of DN and other renal diseases. We hypothesized that the collective action of multiple integrin subtypes may be involved in the development of DN and

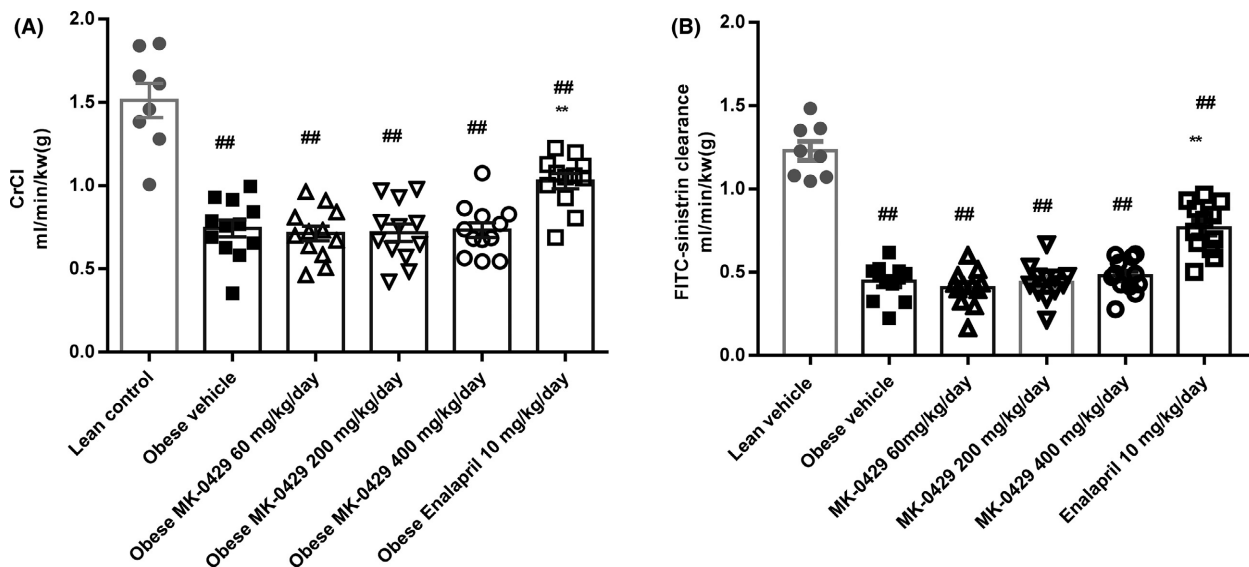


**Figure 4.** (A) Glomerular filtration rate (GFR) estimated by creatinine clearance (CrCl).  $###P < 0.01$ , all obese vehicle versus lean control.  $**P < 0.01$ , enalapril 10 mg/kg/day versus obese vehicle. (one-way ANOVA followed by Tukey). (B) Glomerular filtration rate (GFR) measured by FITC-sinistrin clearance.  $###P < 0.01$ , all obese vehicle versus lean control.  $**P < 0.01$ , enalapril 10 mg/kg/d versus obese vehicle. (one-way ANOVA followed by Tukey).

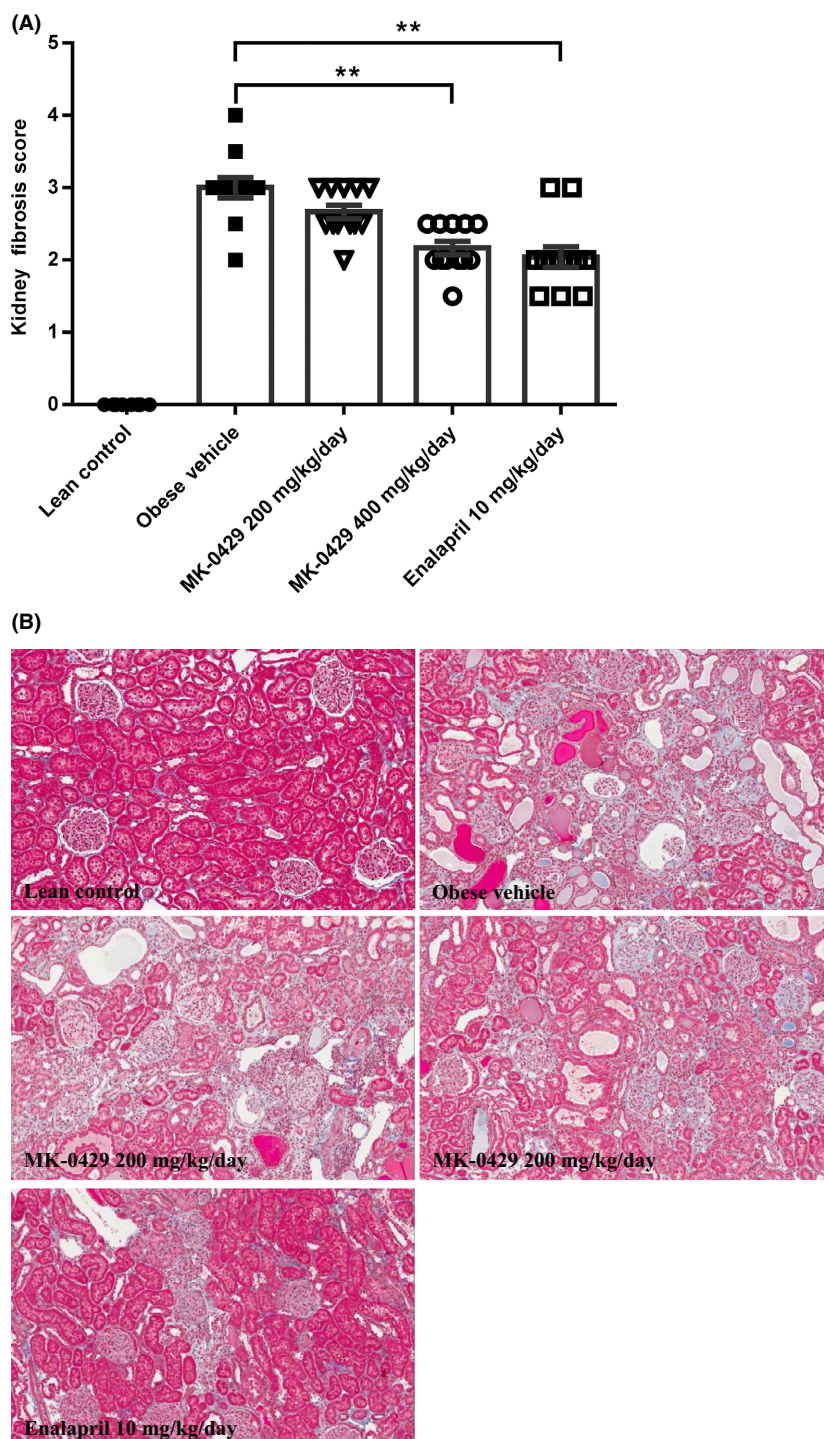


**Figure 5.** (A) Kidney fibrosis scores. Data are mean  $\pm$  SEM ( $n = 8$  for the lean control group,  $n = 12$  for all the obese groups with or without treatment). Both enalapril and MK-0429 400 mg/kg/day significantly decreased kidney fibrosis scores.  $**P < 0.0001$  versus Vehicle. (B) Representative light microscopic findings (10 $\times$ ) showing excessive fibrous tissue occurred in the interstitium in the vehicle group, which was significantly improved by MK-0429 400 mg/kg/day treatment.

a pharmacological approach that targets multiple integrins would lead to meaningful effects on the disease. We found that the expression of RGD integrins was

upregulated in multiple renal cell types, including HPKF, RPTEC, podocytes, and NHMC. Consistent with the cellular findings, we also demonstrated increased renal

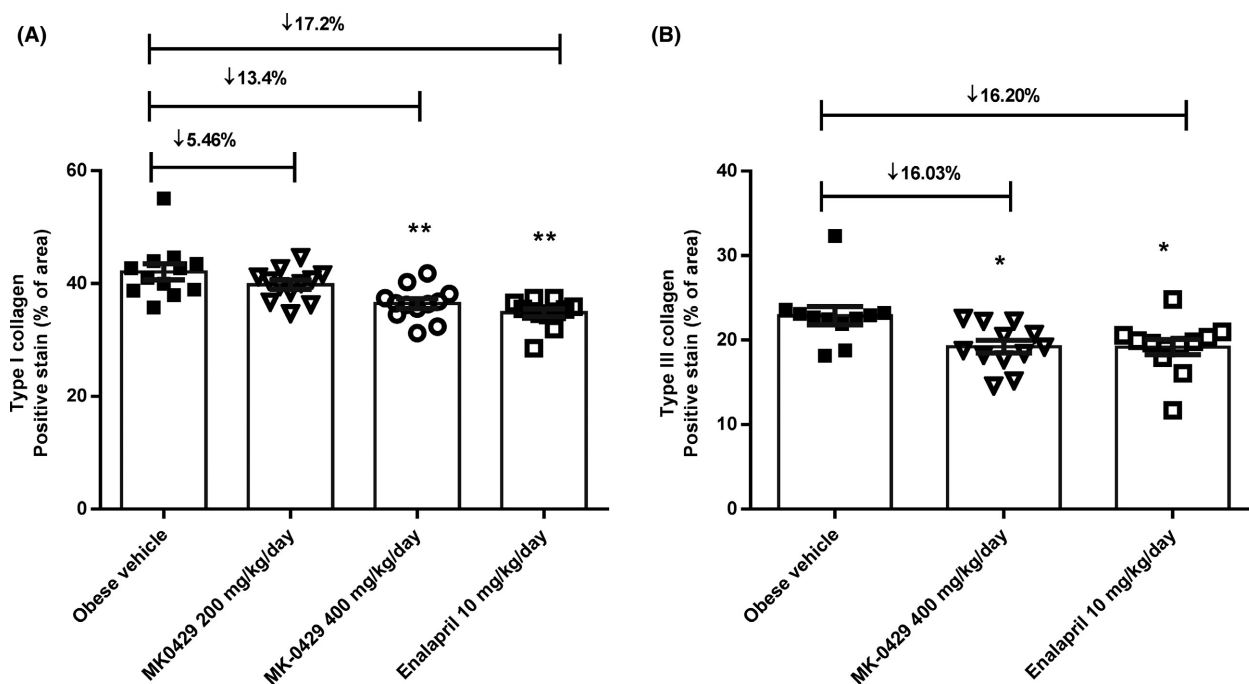


**Figure 6.** (A) Kidney collagen I protein expression assessed by immunohistochemistry (IHC). \*\*\**P* < 0.01 versus obese vehicle. (B) Kidney collagen III protein expression assessed by immunohistochemistry (IHC). \**P* < 0.01 versus obese vehicle.

expression of  $\alpha v\beta 1$ ,  $\alpha v\beta 3$ ,  $\alpha v\beta 5$ , and  $\alpha v\beta 6$  integrins in the ZSF1 rat model. The increased expression of multiple RGD integrins correlates with the injury state of DN, suggesting that these integrins likely play a critical role in the molecular mechanisms underlying DN. As previously reported,  $\alpha v\beta 6$  integrin was restricted to epithelial cells and was further induced by TGF- $\beta$  stimulation. A recent study has shown that  $\alpha v\beta 1$  is highly expressed in activated fibroblasts and modulates lung and liver fibrosis (Reed et al. 2015). In this study, we found that  $\alpha v\beta 1$  is also expressed in RPTEC, podocytes, and NHMC in response to TGF- $\beta$ , which is suggestive of a potentially broader role of  $\alpha v\beta 1$ .

Consistent with the *in vitro* characterization of MK-0429, we demonstrated that MK-0429 is active in functional assays that represent various aspects of the pathophysiology of DN. We initially focused on the role of MK-0429 in the context of podocyte health. Podocytes maintain the glomerular filtration barrier in the kidney. Injury to podocytes leads to actin cytoskeleton reorganization, foot process effacement, and leakage of albumin to the urine (Reiser and Sever 2013). Podocyte injury and dysfunction are hallmarks for a number of proteinuric glomerular diseases including DN (Kriz et al. 1998). Members of the integrin family, such as  $\alpha v\beta 3$ , have been shown to modulate podocyte “plasticity” by reorganizing the actin cytoskeleton and impacting foot process formation (Faul et al. 2008; Pozzi and Zent 2013). We

demonstrated that MK-0429 indeed effectively inhibits podocyte motility *in vitro*. Our observation suggests that MK-0429 affects podocyte actin cytoskeleton reorganization likely through  $\alpha v\beta 3$ , a known vitronectin receptor (Charo et al. 1990). We speculate that modulation of the cytoskeleton rearrangement in podocytes may be the potential mechanism underlying MK-0429 anti-proteinuric effect observed *in vivo*. Electron microscopic analysis of podocyte morphology would be valuable to verify this hypothesis.

A number of pathophysiological processes, such as tubular injury, macrophage infiltration, inflammation, and fibrosis, contribute to the progression of DN to end-stage renal disease (ESRD) (Thomas et al. 2015; Breyer and Susztak 2016). Specifically, tubulointerstitial fibrosis, characterized as excessive accumulation of ECM in the parenchyma, is a hallmark of ESRD and strongly associates with renal function decline in patients with chronic kidney diseases (CKD) (Arora and Singh 2013; Duffield 2014; Thomas et al. 2015). RGD-binding integrins contribute to tissue fibrosis by activating latent TGF- $\beta$  and modulating ECM synthesis. As a potent pan- $\alpha v$  integrin inhibitor, MK-0429 has demonstrated dose-dependent inhibition of fibrosis marker gene expression in kidney fibroblasts. Those fibrosis markers are direct downstream targets of TGF- $\beta$  signaling. Our results suggest that MK-0429 exerts strong anti-fibrotic effects likely due to the modulation of some or all of the latent TGF- $\beta$  -binding

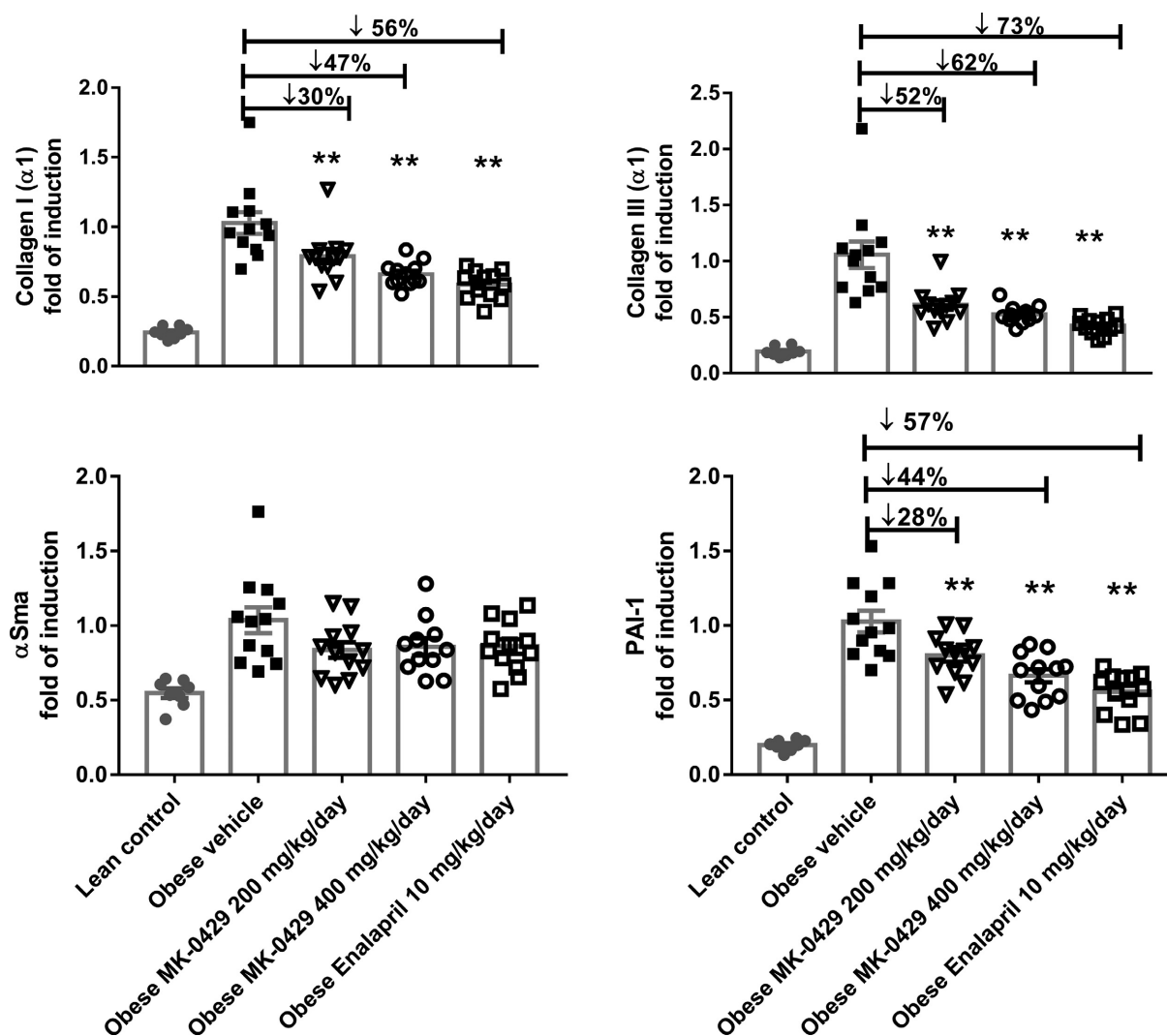


**Figure 7.** Kidney fibrosis marker gene expression assessed by RT-PCR.  $**P < 0.01$  versus obese vehicle. Col IA1, Collagen type I alpha-1 chain; Col IIIA1, Collagen type III alpha-1 chain;  $\alpha$ SMA,  $\alpha$ -smooth muscle actin; PAI-1, plasminogen activator inhibitor-1.

integrins, including  $\alpha v\beta 1$ ,  $\alpha v\beta 6$ , and  $\alpha v\beta 8$ . Recently, an  $\alpha v\beta 1$  inhibitor, compound 8 (C8) has been shown to have anti-fibrotic properties in pulmonary and hepatic fibrosis models (Reed et al. 2015). More recently, C8 was also shown to be protective in the UUU and adenine induced renal injury models (Chang et al. 2017). Our data suggest that MK-0429-dependent inhibition of  $\alpha v\beta 1$  is partially responsible for the anti-fibrotic effects in vivo; however, it is likely that inhibition of  $\alpha v\beta 6$ ,  $\alpha v\beta 8$ , and potentially  $\alpha 5\beta 1$  are also involved in this process. We speculate that cross-talk between the RGD integrins is important in the response to renal injury and the progression of fibrosis.

The ZSF-1 rat is an established superb model of DN (Tofovic et al. 2000; Zhang et al. 2007). It is one of the

few models that meet the criteria of rodent models of DN (Brosius et al. 2009). In this study, chronic treatment with MK-0429 for 28 weeks resulted in anti-fibrotic effect comparable to enalapril. The anti-fibrotic effect of MK-0429 was further confirmed by decreased collagen deposition. Key genes involved in TGF- $\beta$  signaling pathway were significantly reduced in a dose-dependent manner. It is important to note that the dose of enalapril used in our study is estimated to be roughly 3–10-fold over the clinically relevant dose. This high dose leads to profound hemodynamic effects (Boustany-Kari et al. 2016) that are likely the primary mechanism for the immediate drop in proteinuria and the improvement in GFR observed throughout the study. In contrast, ZSF1 rats treated with MK-0429 display late onset reduction in proteinuria

suggesting that the underlying mechanism is likely independent of hemodynamics. The precise cellular and molecular mechanisms of efficacy is not known, however, it is likely to occur via remodeling effects either at the podocyte level and/or via suppression of fibrosis in the interstitium. Analysis of key molecular pathways involved in this process is currently under investigation.

Although much has been learned of the molecular mechanisms underlying renal fibrogenesis, it remained to be seen if these molecular mechanisms would translate to clinical application relating to renal function. As observed in this study, although the reduction in proteinuria was significant with MK-0429 treatment, GFR levels were unchanged. The possibility that longer duration of treatment will be required for further remodeling and subsequently functional benefits remains an option.

CKD is a common comorbidity in patients with type 2 diabetes mellitus (T2DM) and both conditions are increasing in prevalence (Thomas et al. 2015). Increased albuminuria and decreased GFR correlate with cardiovascular and renal events in patients with T2DM (Ninomiya et al. 2009). Current therapies are limited to angiotensin-converting enzyme inhibitors and angiotensin receptor blockers that were approved over 20 years ago. Since then important advances have been made in basic and clinical nephrology research and several mechanisms are currently being tested at different stages of clinical development. A therapeutic agent targeting both renal fibrosis and podocyte health could potentially delay the disease progression and offer synergetic benefits when combined with standard-of-care agents. However, our data demonstrated that targeting multiple integrin subtypes by MK-0429 only led to a modest reduction in proteinuria and renal fibrosis without preserving GFR and improving glomerular and tubular histological changes, which makes this approach for DN therapy rather challenging. Whether a combination of MK-0429 with enalapril will further reduce collagen accumulation, improve tubulointerstitial fibrosis, and glomerulosclerosis, and provide a greater protection on renal function require further investigation.

In summary, the complexity of the integrin biology and their role in the progression of the disease suggest that a pharmacological inhibitor of multiple integrin subtypes might be necessary to lead to meaningful effects in delaying the progression of DN. Further investigation will be required to identify the optimal balance and the relative contribution of the integrin subtypes to the progression of the disease. A small molecule integrin modulator targeting the optimal combination of integrins might serve as a potentially ideal therapy in combination with standard-of-care for patient with DN.

## Acknowledgement

The authors thank S. Gurkan, D. Seiffert and L. Thi Duong for their helpful suggestions on the manuscript.

## Author Contributions

X. Zhou, J. Zhang, M. Hoek, J. M. Cox, L. Ma, D. E. Kelley, and S. Pinto participated in research design. X. Zhou, J. Zhang, R. Haimbach, W. Zhu, R. Mayer-Ezell, M. Garcia-Calvo, E. Smith, O. Price, Y. Kan, E. Zycband, Y. Zhu, and L. Ma conducted experiments and data analysis. J. M. Cox contributed new reagents or analytic tools. X. Zhou, J. Zhang, M. Hoek, L. Ma, D. E. Kelley, and S. Pinto wrote or contributed to the writing of the manuscript.

## Recommended Section

Drug Discovery and Translational Medicine.

## Disclosure

All authors were employees of Merck & Co., Inc., at the time when the work was performed and may hold stock or stock options of the company.

## References

- Afkarian M, Sachs MC, Kestenbaum B, Hirsch IB, Tuttle KR, Himmelfarb J, et al. (2013). Kidney disease and increased mortality risk in type 2 diabetes. *J Am Soc Nephrol* 24: 302–308.
- Akhurst RJ, Hata A (2012). Targeting the TGF $\beta$  signaling pathway in disease. *Nat Rev Drug Discov* 11: 790–811.
- Arora MK, Singh UK (2013). Molecular mechanisms in the pathogenesis of diabetic nephropathy: an update. *Vascul Pharmacol* 58: 259–271.
- Boustany-Kari CM, Harrison PC, Chen H, Lincoln KA, Qian HS, Clifford H, et al. (2016). A soluble guanylate cyclase activator inhibits the progression of diabetic nephropathy in the ZSF1 rat. *J Pharmacol Exp Ther* 356: 712–719.
- Breyer MD, Susztak K (2016). The next generation of therapeutics for chronic kidney disease. *Nat Rev Drug Discov* 15: 568–588.
- Brosius FC III, Alpers CE, Bottinger EP, Breyer MD, Coffman TM, Gurley SB, et al. ; Animal Models of Diabetic Complications Consortium (2009). Mouse models of diabetic nephropathy. *J Am Soc Nephrol* 20: 2503–2512.
- Chang Y, Lau WL, Jo H, Tsujino K, Gewin L, Reed NI, et al. (2017). Pharmacologic blockade of  $\alpha v \beta 1$  integrin ameliorates renal failure and fibrosis in vivo. *J Am Soc Nephrol* 28:1998–2005.

- Charo IF, Nannizzi L, Smith JW, Cheresch DA (1990). The vitronectin receptor alpha v beta 3 binds fibronectin and acts in concert with alpha 5 beta 1 in promoting cellular attachment and spreading on fibronectin. *J Cell Biol* 111: 2795–2800.
- Coleman PJ, Brashear KM, Askew BC, Hutchinson JH, McVean CA, Duong LT, et al. (2004). Nonpeptide alphavbeta3 antagonists. Part 11: discovery and preclinical evaluation of potent alphavbeta3 antagonists for the prevention and treatment of osteoporosis. *J Med Chem* 47: 4829–4837.
- Cowley AW Jr, Ryan RP, Kurth T, Skelton MM, Schock-Kusch D, Gretz N (2013). Progression of glomerular filtration rate reduction determined in conscious Dahl salt-sensitive hypertensive rats. *Hypertension* 62: 85–90.
- Ding Y, Choi ME (2014). Regulation of autophagy by TGF- $\beta$ : emerging role in kidney fibrosis. *Semin Nephrol* 34: 62–71.
- Duffield JS (2014). Cellular and molecular mechanisms in kidney fibrosis. *J Clin Invest* 124: 2299–2306.
- Faul C, Donnelly M, Merscher-Gomez S, Chang YH, Franz S, Delfgaauw J, et al. (2008). The actin cytoskeleton of kidney podocytes is a direct target of the antiproteinuric effect of cyclosporine A. *Nat Med* 14: 931–938.
- Gentile G, Mastroiuda D, Ruggerenti P, Remuzzi G (2014). Novel effective drugs for diabetic kidney disease? or not? *Expert Opin Emerg Drugs* 19: 571–601.
- Henderson NC, Sheppard D (2013). Integrin-mediated regulation of TGF $\beta$  in fibrosis. *Biochim Biophys Acta* 1832: 891–896.
- Henderson NC, Arnold TD, Katamura Y, Giacomini MM, Rodriguez JD, McCarty JH, et al. (2013). Targeting of  $\alpha v$  integrin identifies a core molecular pathway that regulates fibrosis in several organs. *Nat Med* 19: 1617–1624.
- Horan GS, Wood S, Ona V, Li DJ, Lukashev ME, Weinreb PH, et al. (2008). Partial inhibition of integrin alpha(v)beta6 prevents pulmonary fibrosis without exacerbating inflammation. *Am J Respir Crit Care Med* 177: 56–65.
- Hutchinson JH, Halczenko W, Brashear KM, Breslin MJ, Coleman PJ, Duong LT, et al. (2003). Nonpeptide alphavbeta3 antagonists. In vitro and in vivo evaluation of a potent alphavbeta3 antagonist for the prevention and treatment of osteoporosis. *J Med Chem* 46: 4790–4798.
- Hynes RO (2002). Integrin: bidirectional, allosteric signaling machines. *Cell* 110: 673–687.
- Jin DK, Fish AJ, Wayner EA, Mauer M, Setty S, Tsilibary E, et al. (1996). Distribution of integrin subunits in human diabetic kidneys. *J Am Soc Nephrol* 7: 2636–2645.
- Kindt F, Hammer E, Kemnitz S, Blumenthal A, Klemm P, Schlüter R, et al. (2017). A novel assay to assess the effect of pharmaceutical compounds on the differentiation of podocytes. *Br J Pharmacol* 174: 163–176.
- Kitamura H, Cambier S, Somanath S, Barker T, Minagawa S, Markovics J, et al. (2011). Mouse and human lung fibroblasts regulate dendritic cell trafficking, airway inflammation, and fibrosis through integrin  $\alpha v \beta 8$ -mediated activation of TGF- $\beta$ . *J Clin Invest* 121: 2863–2875.
- Kriz W, Gretz N, Lemley KV (1998). Progression of glomerular diseases: is the podocyte the culprit? *Kidney Int* 54: 687–697.
- Ma LJ, Yang H, Gaspert A, Carlesso G, Barty MM, Davidson JM, et al. (2003). Transforming growth factor-beta-dependent and -independent pathways of induction of tubulointerstitial fibrosis in beta6(-/-) mice. *Am J Pathol* 163: 1261–1273.
- Maile LA, Busby WH, Gollahon KA, Flowers W, Garbacik N, Garbacik S, et al. (2014a). Blocking ligand occupancy of the  $\alpha V \beta 3$  integrin inhibits the development of nephropathy in diabetic pigs. *Endocrinology* 155: 4665–4675.
- Maile LA, Gollahon K, Wai C, Dunbar P, Busby W, Clemmons D (2014b). Blocking  $\alpha V \beta 3$  integrin ligand occupancy inhibits the progression of albuminuria in diabetic rats. *J Diabetes Res* 2014: 421827.
- Munger JS, Huang X, Kawakatsu H, Griffiths MJ, Dalton SL, Wu J, et al. (1999). The integrin alpha v beta 6 binds and activates latent TGF beta 1: a mechanism for regulating pulmonary inflammation and fibrosis. *Cell* 96: 319–328.
- Murphy MG, Cerchio K, Stoch SA, Gottesdiener K, Wu M, Recker R; L-000845704 Study Group (2005). Effect of L-000845704, an alphaVbeta3 integrin antagonist, on markers of bone turnover and bone mineral density in postmenopausal osteoporotic women. *J Clin Endocrinol Metab* 90: 2022–2028.
- Ninomiya T, Perkovic V, deGalan BE, Zoungas S, Pillai A, Jardine M, et al. ; ADVANCE Collaborative Group (2009). Albuminuria and kidney function independently predict cardiovascular and renal outcomes in diabetes. *J Am Soc Nephrol* 20:1813–1821.
- Pozzi A, Zent R (2013). Integrins in kidney disease. *J Am Soc Nephrol* 24: 1034–1039.
- Reed NI, Jo H, Chen C, Tsujino K, Arnold TD, DeGrado WF, et al. 2015. The  $\alpha v \beta 1$  integrin plays a critical in vivo role in tissue fibrosis. *Sci Transl Med* 7:1–8.
- Reiser J, Sever S (2013). Podocyte biology and pathogenesis of kidney disease. *Annu Rev Med* 64: 357–366.
- Rosenthal MA, Davidson P, Rolland F, Campone M, Xue L, Han TH, et al. (2010). Evaluation of the safety, pharmacokinetics and treatment effects of an alpha(nu)beta(3) integrin inhibitor on bone turnover and disease activity in men with hormone-refractory prostate cancer and bone metastases. *Asia Pac J Clin Oncol* 6: 42–48.
- Schock-Kusch D, Xie Q, Shulhevich Y, Hesser J, Stsepankou D, Sadick M, et al. (2011). Transcutaneous assessment of renal

function in conscious rats with a device for measuring FITCsinistrin disappearance curves. *Kidney Int* 79: 1254–1258.

Thomas MC, Brownlee M, Susztak K, Sharma K, Jandeleit-Dahm KA, Zoungas S, et al. (2015). Diabetic kidney disease. *Nat Rev Dis Primers* 1: 15018.

Tofovic S, Kusaka H, Kost C Jr, Bastacky S (2000). Renal function and structure in diabetic, hypertensive, obese ZDFxSHHF-hybrid rats. *Ren Fail* 22: 387–406.

USRDS ADR (2014). United State Renal Data System, the 2014 Annual Data Report.

Wei C, Möller CC, Altintas MM, Li J, Schwarz K, Zacchigna S, et al. (2008). Modification of kidney barrier function by the urokinase receptor. *Nat Med* 14: 55–63.

Zhang X, Jia Y, Jackson EK, Tofovic SP (2007). 2-Methoxyestradiol and 2-ethoxyestradiol retard the progression of renal disease in aged, obese, diabetic ZSF1 rats. *J Cardiovasc Pharmacol* 49: 56–63.

Zhou X, Crook MF, Sharif-Rodriguez W, Zhu Y, Ruben Z, Pan Y, et al. (2011). Chronic antagonism of the mineralocorticoid receptor ameliorates hypertension and end organ damage in a rodent model of salt-sensitive hypertension. *Clin Exp Hypertens* 33: 538–547.

Zhou X, Zhang Z, Shin MK, Horwitz SB, LeVorse JM, Zhu L, et al. (2013). Heterozygous disruption of renal outer medullary potassium channel in rats is associated with reduced blood pressure. *Hypertension* 62: 288–294.

## Supporting Information

Additional Supporting Information may be found online in the supporting information tab for this article:

**Figure S1.** (A) MK-0429 dose-titration in solid-phase ELISA assay. Serial threefold dilution of MK-0429 was added to each integrin-ligand reaction, and DMSO was shown as the negative control. (B) Thermal shift assay reveals distinct selectivity of MK-0429. The change in melting temperature ( $\Delta T_m$ ) was calculated by comparing the  $T_m$  after the addition of MK-0429 or DMSO (negative control) to each integrin. (C) Densitometry graph of integrin expression in human primary kidney cells following coimmunoprecipitation and Sally Sue simple western analyses. The chemiluminescent signal of each integrin was normalized against the signal of GAPDH in total cell lysate.